

Topical Review

Quadrupole matrix element zeros and their effect on photoelectron angular distributions

L.A. LaJohn^{a,*}, S.T. Manson^b, R.H. Pratt^a

^a Department of Physics and Astronomy, University of Pittsburgh, Pittsburgh, PA 15260, USA

^b Department of Physics and Astronomy, Georgia State University, Atlanta, GA 30303, USA

ARTICLE INFO

Available online 13 November 2009

Keywords:

Zeros

Photoionization

Matrix element

Angular distribution parameter

ABSTRACT

Calculations of the lowest order nondipole photoelectron angular distribution parameters are made for 5s and 6s photoionization of Nd ($Z=60$). The results show a strong dependence upon the locations of the Cooper minima in the dipole and quadrupole photoionization channels.

© 2009 Elsevier B.V. All rights reserved.

1. Introduction

Over the past decade, there have been an increasing number of measurements of nondipole effects in photoelectron angular distributions in the low-energy region, i.e., photon energies of hundreds [1] or even tens of eV [2]. These measurements, along with theoretical calculations [3–6], indicate the importance of the existence of zeros, Cooper minima [7], in dipole and quadrupole matrix elements upon the nondipole parameters of the angular distribution. Dipole Cooper minima (DCM) have been known for some time both experimentally and theoretically, and their appearance over the entire periodic table has been studied extensively [8,9]. Quadrupole Cooper minima (QCM) were postulated theoretically some time ago [10], but only recently have they been confirmed experimentally [11]. However, no systematic studies have been made of the QCM.

To remedy that situation, we have initiated a project to study QCM's for the ground states of all of the elements of the periodic table. In this paper, we present the results of a study of 5s and 6s photoionization of Nd ($Z=60$) at the relativistic central-field approximation level, to provide a guide to how the various zeros affect the nondipole angular distribution parameters; ns states were chosen because the effects of the minima show up most clearly for ns states [5,11]. In addition, by choosing a target of reasonably high Z , information on the influence of relativistic effects can also be gleaned.

2. Theory

For linearly polarized incident radiation, the differential photoionization cross-section, including dipole–dipole and dipole–quadrupole interferences, for a given subshell is given by [4]

$$d\sigma_i/d\Omega = \sigma_i/4\pi[1 + \beta P_2(\cos\theta) + (\delta + \gamma \cos^2\theta)\sin\theta \cos\varphi] \quad (1)$$

where σ is the angle-integrated cross-section, β the dipole anisotropy parameter, $P_2(\cos\theta) = (3\cos^2\theta - 1)/2$, and δ and γ first-order nondipole asymmetry parameters. The coordinate axes have the positive x -axis along the direction of the photon propagation vector, the z -axis along the photon polarization vector, and θ and φ are the polar and azimuthal angles of the photoelectron momentum vector. The dipole angular distribution parameter β depends only on ratios of dipole matrix elements, along with cosines of phase-shift differences [12], while δ and γ depend upon dipole and quadrupole matrix elements, along with cosines of their phase-shift differences [4]. For the special case of the photoionization of initial ns states, within a central-field model, $\beta=2$. In addition, $\delta=0$ nonrelativistically [4] and is very close to zero in our relativistic results so we discuss it no further; similar results have been found in other cases [13,14].

The parameter γ , within a relativistic context, is given by

$$\gamma = \frac{3k}{5} \frac{6D_{3/2}Q_{3/2}\cos\Delta_{3/2,3/2} + 5D_{1/2}Q_{5/2}\cos\Delta_{1/2,5/2} + 4D_{3/2}Q_{5/2}\cos\Delta_{3/2,5/2}}{D_{1/2}^2 + 2D_{3/2}^2} \quad (2)$$

where D_j and Q_j are the absolute values of the radial parts of the relativistic dipole $ns \rightarrow \epsilon p_j$ and quadrupole $ns \rightarrow \epsilon d_j$ photoionization amplitudes, respectively, $\Delta_{j,j'} = \delta_j^D - \delta_{j'}^Q$, the phase shift differences between dipole and quadrupole channels, and k is the photon wave number ($=\omega/c$ where ω is photon energy). In the nonrelativistic limit, where the matrix elements and their phases

* Corresponding author.

E-mail address: lal18@pitt.edu (L.A. LaJohn).

are independent of j , the expression for γ reduces to [3,4]

$$\gamma = 3k \frac{Q}{D} \cos \Delta \quad (3)$$

essentially a ratio of quadrupole to dipole matrix elements to within a multiplicative factor.

The relativistic dipole and quadrupole matrix elements were obtained using Dirac–Slater central field wave functions for initial discrete and final continuum states. The details of the calculation have been described earlier [3,9].

3. Results and discussion

The results of calculations for the case of 5s photoionization are shown in Fig. 1. The dipole matrix elements, seen in Fig. 1a, show that relativistic effects play a significant role; the $p_{3/2}$ channel exhibits a zero right about at threshold, while for the $p_{1/2}$ channel, there is no hint of a zero in the continuum. This is evidently due to that the $\epsilon p_{1/2}$ wave function is more compact than the $\epsilon p_{3/2}$. For the quadrupole matrix elements (Fig. 1b), both relativistic channels are found to have a zero right about 80 eV. The very small splitting of the quadrupole zeros occurs because

spin–orbit interaction is much smaller in d-states than in p-states owing to the centrifugal barrier that keeps the d-states out of the inner region where the spin–orbit interaction is largest. The resulting nondipole parameter γ , seen in Fig. 1c, reflects the location of these zeros. Since the quadrupole zeros are at the quite close to each other, it is evident from Eq. (3) that γ must have a zero at the same energy; that is exactly what is seen. The dipole channels differ so the situation near the DCM cannot be analyzed so simply. All three terms of Eq. (2) contribute, and the result is also influence by the cosine factors. But generally, γ shows a maximum in absolute value near the $p_{3/2}$ DCM, but not exactly at that point owing to the complicated influence of the other terms in Eq. (2).

The situation is somewhat different for 6s photoionization, as seen in Fig. 2. Both $p_{3/2}$ and $p_{1/2}$ channels (Fig. 2a) are seen have DCM in the continuum, in the 10 eV region, split by about 10 eV owing to relativity; as expected, the $p_{3/2}$ zero is at higher energy; the difference in the positions of the DCM's between 5s and 6s is due to the different extent and shape of the 6s wave function compared to 5s. In Fig. 2b, it is seen that both quadrupole channels exhibit zeros and at roughly the same energy (about 50 eV), just as in the 5s case, although here the zeros are at significantly lower energy than for 5s. These matrix elements

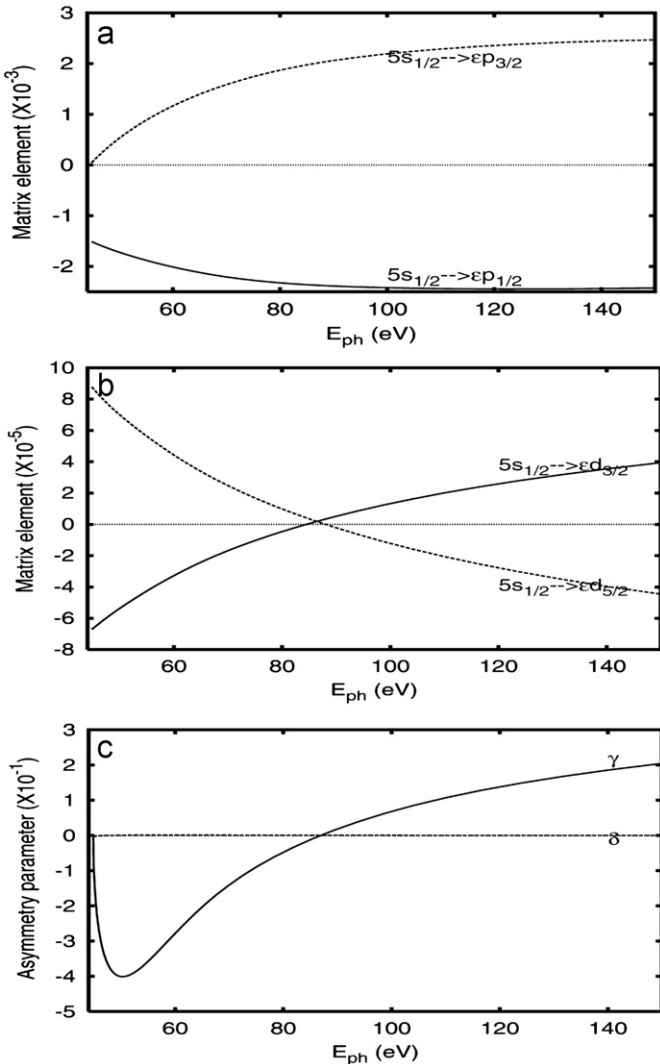


Fig. 1. Photoionization of the 5s subshell of Nd ($Z=60$): (a) radial dipole matrix elements; (b) radial quadrupole matrix elements; (c) nondipole photoelectron angular distribution asymmetry parameter γ .

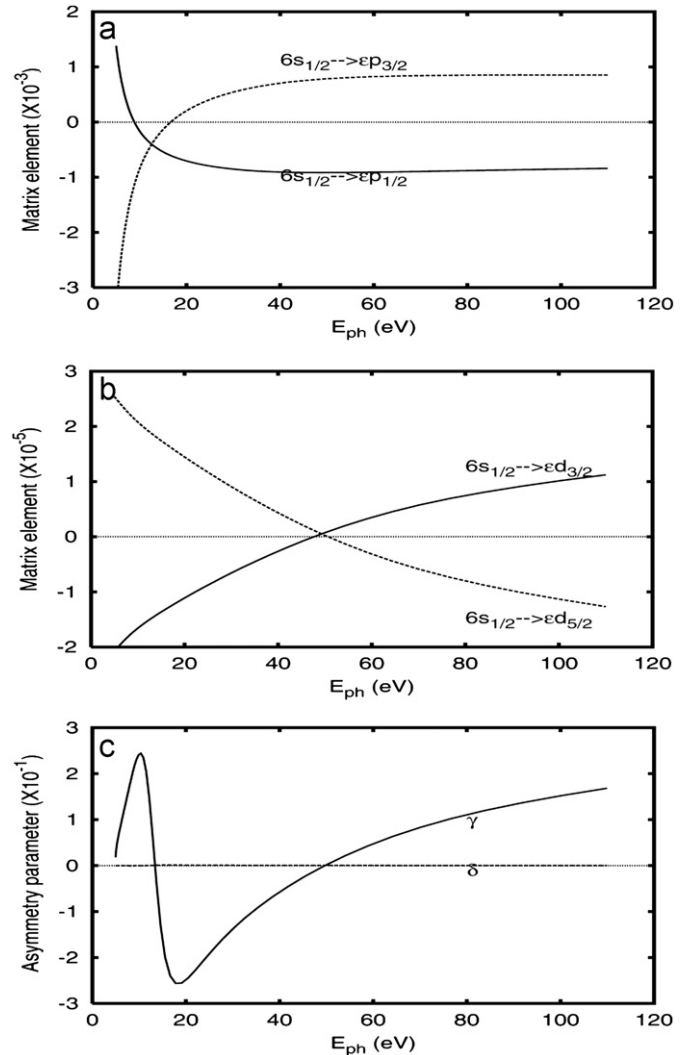


Fig. 2. As Fig. 1 but for the 6s subshell.

translate to the γ parameter shown in Fig. 2c where it is seen that γ is zero around 50 eV where the QCM are; there is also a zero around 10 eV which evidently has nothing to do with QCM's. Furthermore, at low energy the shape of γ is clearly completely different than in the 5s case. This occurs because near threshold, there are maxima in the absolute value of γ in the vicinity of each of the DCM's; where the $p_{1/2}$ term dominates the expression for γ , near 10 eV, the maximum is positive; where the $p_{3/2}$ term dominates the expression, near 20 eV, the maximum is negative, just as in the 5s case; the zero in γ between the two maxima is a consequence of the two terms in the expression for γ being more or less equal and opposite.

Note that there are three types of quadrupole matrix element zeros (QMZ). Those that occur at photon energy $E\rho < 1$ keV are designated as Type I and are the Cooper minima discussed above. They occur for transitions in which the change in orbital angular momentum $\Delta l = l_b - l_c$ (l_b and l_c are the orbital angular momenta of the bound and continuum states, respectively) are 2 and -2 , and the change in total angular momentum, $\Delta j = j_b - j_c$ is 2, 1, 0, -1 , and -2 . There is a second type of QMZ that occurs in the energy range $1 \text{ keV} < E\rho < 50 \text{ keV}$, which we designate as Type II [10,15], and a third type which occurs at relativistic energies $E\rho > 50 \text{ keV}$, designated as Type III. [16]. The Type II QMZ, unlike Type I, only occur for Δl of 2 and Δj of 2 and 1. The QMZ are similar to their dipole counterparts [17], only occur in Δl of 2 and 0 and Δj of 1, 0, and -1 transitions. These Type II and Type III zeros should have observable consequences as well.

4. Conclusions

In all cases the γ parameter vanishes around the QCM and reaches a maximum absolute value around the DCM. Relativistic (spin-orbit) splittings modify these conclusions slightly, as

demonstrated above. It is also evident that while QCM's lead to zeros in γ , zero's in γ do not necessarily infer QCM's, as seen for the 6s case. Finally, it is to be emphasized that the magnitudes of the nondipole parameter γ predicted are large enough to be studied experimentally. Such measurements can shed light on the existence and location of QCM's and DCM's along with information on the relativistic splitting of these minima, information which is essentially impossible to glean from integrated cross-section measurements.

Acknowledgment

This work was supported by NSF and DOE, Office of Basic Sciences.

References

- [1] O. Hemmers, et al., J. Phys. B 30 (1997) L727.
- [2] B. Krässig, et al., Phys. Rev. Lett. 88 (2002) 203002.
- [3] A. Bechler, R.H. Pratt, Phys. Rev. A 39 (1990) 1774; A. Bechler, R.H. Pratt, Phys. Rev. A 42 (1990) 6400 and references therein.
- [4] J.W. Cooper, Phys. Rev. A 47 (1993) 1841 and references therein.
- [5] W.R. Johnson, K.T. Cheng, Phys. Rev. A 63 (2001) 022504.
- [6] V.K. Dolmatov, S.T. Manson, Phys. Rev. Lett. 83 (1999) 939.
- [7] J.W. Cooper, Phys. Rev. 128 (1962) 681.
- [8] S.T. Manson, Phys. Rev. A 31 (1985) 3698.
- [9] R.Y. Yin, R.H. Pratt, Phys. Rev. A 35 (1987) 1149.
- [10] M.S. Wang, Young Soon Kim, R.H. Pratt, A. Ron, Phys. Rev. A 25 (1982) 857.
- [11] P.C. Deshmukh, et al., J. Phys. B 41 (2008) 021002.
- [12] S.T. Manson, A.F. Starace, Rev. Mod. Phys. 54 (1982) 389.
- [13] A. Derevianko, W.R. Johnson, K.T. Cheng, At. Data Nucl. Data Tables 73 (1999) 153.
- [14] M.B. Trzhaskovskaya, V.K. Nikulin, V.I. Nefedov, V.G. Yarzhevsky, J. Phys. B 34 (2001) 3221 and references therein.
- [15] Y.S. Kim, R.H. Pratt, A. Ron, H.K. Tseng, Phys. Rev. A 22 (1980) 567.
- [16] L.A. Lajohn, R.H. Pratt, Rad. Phys. and Chem. 71 (2004) 665.
- [17] L.A. Lajohn, R.H. Pratt, Phys. Rev. A 67 (2003) 032701.